Available online at www.sciencedirect.com
ScienceDirect
Trans. Nonferrous Met. Soc. China 25(2015) 2884−2892
Transactions of Nonferrous Metals Society of China
www.tnmsc.cn

Effects of pouring temperature and cylinder temperature on microstructures and mechanical properties of rheomoulding AZ91D alloy

Ming-fan QI[1], Yong-lin KANG[1], Bing ZHOU[1], Guo-ming ZHU[1], Huan-huan ZHANG[1], Yang-de LI[2]

1. School of Materials Science and Engineering, University of Science and Technology Beijing, Beijing 100083, China;
2. Dongguan EONTEC Co., Ltd., Dongguan 523662, China

Received 5 August 2014; accepted 17 June 2015

Abstract: An advanced rheomoulder, which is a device in the integration of melting metal, storage, slurry preparation, transportation and injection forming, was introduced and used to manufacture rheomoulding AZ91D alloy. Effects of pouring temperature and cylinder temperature on microstructures and mechanical properties of rheomoulding AZ91D alloy were investigated. The results show that the process can obtain such rheomoulding AZ91D in which primary α-Mg particles are fine, spherical and uniformly distributed in the matrix. With the decrease of pouring temperature, the morphology of primary α-Mg particles changes from coarse rosette-like to fine spherical shape gradually. As the cylinder temperature decreases, the average size of primary α-Mg particles decreases firstly and then substantially maintains stable while the sphericity and solid fraction increase continuously. Also, decreasing pouring temperature or cylinder temperature properly contributes to improving mechanical properties of rheomoulding AZ91D for the refinement of α-Mg particles and the decrease of porosity fraction. Furthermore, rheomoulding AZ91D performs much better than thixomoulding, rheo-diecasting and high pressure die-casting (HPDC) in terms of mechanical properties. Compared with HPDC, the tensile strength, yield strength and elongation are increased by 27.8%, 15.7% and 121%, respectively.
Key words: AZ91D alloy; rheomoulding; pouring temperature; cylinder temperature; mechanical properties

1 Introduction

Mg alloy is the lightest metal material used in engineering application with a series of unique properties, such as light weight, high specific strength and specific stiffness, excellent damping property, good thermal conductivity and easy recycle. Thus, it is regarded as a kind of green environmental protection materials in the 21st century, and it will become the crucial material for automotive and 3C (computers, communications and consumer electronics) industries. At present, the study of Mg alloy has become a global issue [1−3].

Mg alloy forming methods mainly include high pressure die-casting (HPDC), squeeze casting, forging and semisolid forming (SSF), etc. Currently, nearly all applications of Mg alloy parts are provided by HPDC [4]. HPDC has a series of advantages, such as good dimensional stability and high productivity. However, the obvious disadvantage of HPDC is that high mechanical properties parts are very difficult to be achieved for casting defects, such as microporosities and gas porosities [3,5]. Compared with HPDC, SSF parts have advantages of less casting defects, better mechanical properties and superior surface and inner qualities, meanwhile, save energy and improve safety [6,7]. Therefore, SSF is considered as the most promising material forming method in the 21st century [8].

Based on the principle of plastic injection forming, the formation of semisolid injection forming (SSIF) technology is formed and applied to the process of SSF. Thixomoulding and rheomoulding are two basic methods of SSIF. Thixomoulding, a semisolid metal processing technology for producing Mg alloy parts in one step in a single machine, has received great interest in recent years [9,10]. GHOSH et al [11] and TSUKEDA et al [12] carried out the earliest study of thixomoulding technology, and researches on thixomoulding AZ91D, AM60 and AZ61 have been conducted. CZERWINSKI [13−15] have conducted systematic studies on thixomoulding AZ91D, including the selection and use of raw materials, the evolution of

Foundation item: Project (2011CB606302-1) supported by the National Basic Research Program of China; Project (2013AA031001) supported by High-tech Research and Development Program of China
Corresponding author: Yong-lin KANG; Tel: +86-10-62332335; E-mail: kangylin@ustb.edu.cn
DOI: 10.1016/S1003-6326(15)63914-0

microstructures and the variation of mechanical properties as experiment parameters change. Though thixomoulding has made a great progress and the alloys of which show better strength and ductility, there still exist many shortcomings, such as poor wear resistance and short service life of the screw and the cylinder liner which are key components of the thixomoulder [16]. Moreover, using Mg alloy particles as raw materials directly results in the increase of production cost [16,17].

In order to solve problems that exist in thixomoulding and develop a novel technology to form Mg alloy parts with high mechanical properties, an advanced rheomoulder with integrated structure is introduced and used in this work. The rheomoulder, combining the technologies of die-casting and plastic injection forming, is a relatively new process for producing near-net-shape Mg alloy parts in one step. With the low superheat pouring (LSP) technology and the intense shear afforded by the slim long nozzle and runner during injection, semisolid slurry is prepared instead of traditional methods, such as the spiral shear and electromagnetic stirring, which not only protects the equipment from abrasion, but also avoids slurry pollution. Moreover, using Mg alloy rods as raw materials reduces the cost to some extent. However, the relevant study to rheomoulding technology is rare. Launching experimental studies and obtaining experimental results have important guiding significance for the development and application of rheomoulding Mg alloy. An effort was made in this study to make use of the rheomoulder to fabricate phone covers as research object and investigate the effects of pouring temperature and cylinder temperature on microstructures and mechanical properties of rheomoulding AZ91D.

2 Experimental

2.1 Experimental equipment

A NISSEI FMg220−16HM rheomoulder, equipped with a phone cover mold, is shown in Fig. 1, which is an equipment in integration of melting metal, storage, slurry preparation, transportation and injection forming**.** It mainly consists of the following five parts. The first part is the material melting system. The system is suitable to accommodate rod-shaped materials with the sizes of *d*60 mm × 300 mm, which are constantly melted in the melting barrel heated by heating components. The second part is the molten material storage system, which is composed of a upper storage tank and a lower material temperature control barrel. The temperatures of the storage tank and the lower material temperature control barrel are considered to be the melt temperature and pouring temperature, respectively. The third part is the semisolid slurry preparation system. The slurry is prepared in the injection cylinder, which mainly consists of the material measurement room, runner and nozzle. The fourth part is the high-speed injection system which is used to inject the slurry into the mold cavity with high pressure and speed. The fifth part is the injection mold.

2.2 Material and procedures

The experimental material is commercial AZ91D alloy rods with chemical compositions of Al 9.44%, Zn 0.66%, Mn 0.2%, Si 0.03%, Fe 0.001%, Cu 0.004%, Ni 0.001% and Mg balance. Liquidus and solidus are 595 °C and 470 °C, respectively.

In the rheomoulding process, pouring temperature, cylinder temperature, injection speed, die temperature,

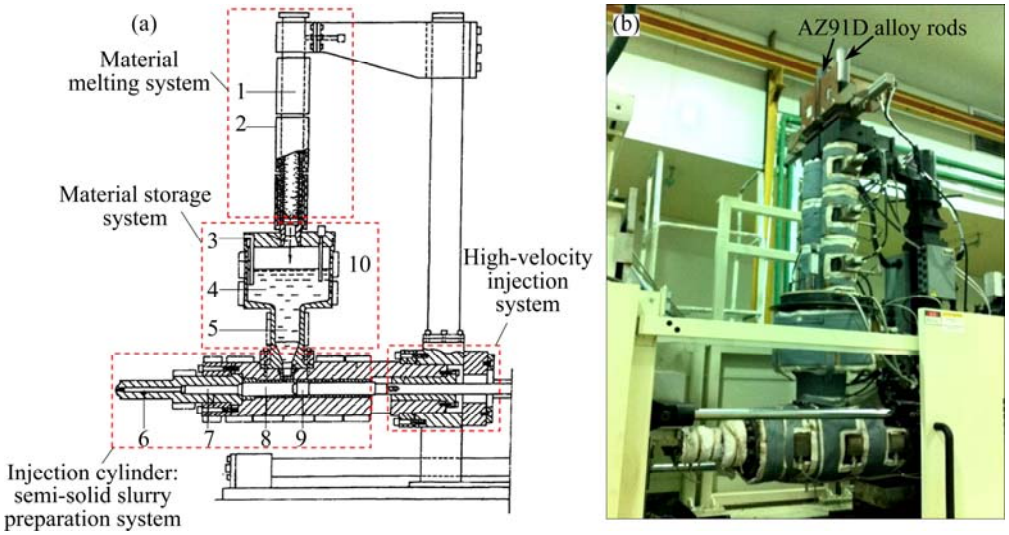

Fig. 1 Schematic diagram (a) and real photo (b) of rheomoulder: 1—Melting barrel; 2—Heating component; 3—Blunt gas injection pipe; 4—Storage tank; 5—Material temperature control barrel; 6—Nozzle; 7—Runner; 8—Material measurement room; 9—Punch; 10—Liquid level detector

injection pressure and forming cycle are the main parameters. In this study, only the pouring temperature and cylinder temperature were altered during experiments. The specific parameters are as follows: melt temperature of 670 °C, pouring temperature of 600−635 °C, cylinder temperature of 595−520 °C, injection speed of 1.6 m/s, mold temperature of 250 °C, injection pressure of 30 MPa and forming cycle of 30 s.

Cross-sections of the samples for optical microscopy observations were roughly ground, finely ground and polished, and then etched by a solution with 4% (volume fraction) nitric acid alcohol. The microstructures were observed by using a NEOPHOT 21 optical microscope and a ZEISS EVO18 scanning electron microscope (SEM) equipped with an energy dispersive X-ray spectrometer (EDX). Rectangular cross-sections of tensile specimens were machined from the middle of phone covers, and the shape and dimensions are shown in Fig. 2. Mechanical properties were measured at room temperature by a MTS810 material testing machine, and the strain rate was 1.0 mm/min. Effects of pouring temperature and cylinder temperature on average size and sphericity of α_1-Mg were investigated by Image Tool image analysis software. The average size of α_1-Mg was symbolized by the equivalent area diameter (D_{eq}):

$$D_{eq}=\left(\sum_{N=1}^{N}\sqrt{4A_N/\pi}\right)\Big/N \tag{1}$$

and the sphericity was recorded as

$$F=\left(\sum_{N=1}^{N}4\pi A_N/P_N^2\right)\Big/N \tag{2}$$

where A_N and P_N are the area and perimeter of the Nth α_1-Mg, respectively, and N is the number of α-Mg. α-Mg is homogeneous and round when F is close to 1.

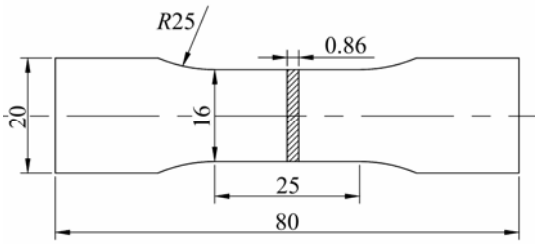

Fig. 2 Schematic diagram of tensile specimens cut from rheomoulding phone covers (unit: mm)

The mass of samples was measured by METTLER AE100 electronic balance with accuracy of 1 mg. According to the Archimedes principle, drainage method was used to measure the density of samples. The density of each sample was the average of five measurement results. The porosity fraction was calculated by the following equation:

$$\phi=\left(1-\frac{\rho}{\rho'}\right)\times 100\% \tag{3}$$

where ϕ is the porosity fraction, ρ is the measured density of sample by the Archimedes principle and ρ' is the standard density of AZ91D alloy.

3 Results and discussion

3.1 Typical microstructure of rheomoulding AZ91D

Figure 3 shows the XRD pattern of rheomoulding AZ91D. Compared with HPDC [18,19] and thixomoulding [10,11], the microstructure of rheomoulding AZ91D also has two phases, including α-Mg and intermetallic compound β-$Mg_{17}Al_{12}$. As indicated in Fig. 3, α-Mg has strong peak in 2θ scanning while β-$Mg_{17}Al_{12}$ has weak peak in 2θ scanning.

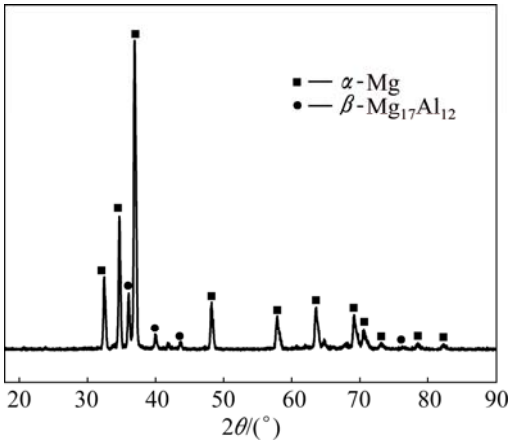

Fig. 3 XRD pattern of rheomoulding AZ91D

Figure 4 shows the typical micrograph and EDX analysis of rheomoulding AZ91D fabricated at pouring temperature of 620 °C and cylinder temperature of 535 °C. It is seen that many spherical, ellipsoidal and rosette-like α_1-Mg particles disperse in liquid matrix (Fig. 4(a)). The matrix is a mixture of α_2-Mg and intermetallic β-$Mg_{17}Al_{12}$, which was also reported by FAN [19] and CZERWINSKI [13]. Meanwhile, some small white round particles are observed at the boundary and inside of a_1-Mg, and their size is about 4 μm (Fig. 4(b)). EDX was used to analyze elemental compositions. As shown in Fig. 4(c), it is mainly composed of Al and Mn, and the measured compositions (mole fraction) are 60.08% Al, 37.07% Mn and 2.81% Mg with the average n(Al)/n(Mn) ratio of 1.62. It is in the composition range of Al_8Mn_5 phase, and can serve as effective nucleation sites for the precipitation temperature within the range of 598−642 °C [20].

Figure 5 shows microstructures of the rheomoulding phone cover at different locations, when pouring temperature is 600 °C and cylinder temperature is 550 °C.

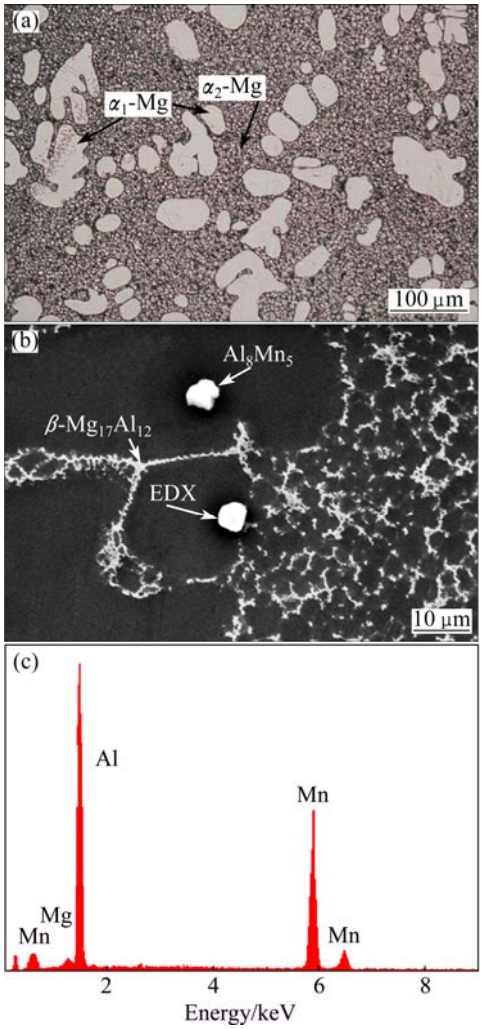

Fig. 4 Typical micrographs (a,b) and EDX analysis (c) of rheomoulding AZ91D

It can be seen that non-dendritic α_1-Mg and numerous very small α_2-Mg phases are uniform throughout the entire casting including the sprue and the shell part, and there are few porosities, manifesting that the process can obtain the rheomoulding AZ91D with typical semisolid features. At sprue, α_1-Mg particles are coarse and granular, and the average size of α_2-Mg is 6.3 μm (Fig. 5(a)). Compared with the sprue, microstructures of the shell part are finer, consisting of spherical and ellipsoidal α_1-Mg and numerous smaller α_2-Mg with the average size of 3.3 μm (Figs. 5(b−f)). This is because that the shell part is thinner, the solidification time is shorter, and as a result, the growth of α-Mg is inhibited.

3.2 Effects of pouring temperature on microstructure and mechanical property

Figure 6 shows microstructures of rheomoulding phone covers under pouring temperatures of 635, 620, 610 and 600 °C with cylinder temperature of 530 °C. The quantitative analysis results of α-Mg and porosity fraction are displayed in Table 1.

From Fig. 6 and Table 1, it is obvious that with the decrease of pouring temperature, the solid fraction increases slightly, the porosity fraction decreases continuously and great changes have taken place in the morphology of α_1-Mg. When the pouring temperature is 635 °C, many coarse rosette-like α_1-Mg can be observed and their average size and sphericity are 53.14 μm and 0.427, respectively. As the temperature decreases, the number of rosette-like α_1-Mg reduces significantly, the average size of α_1-Mg decreases and the sphericity increases. When the pouring temperature decreases to 600 °C, numerous fine spherical α_1-Mg particles are

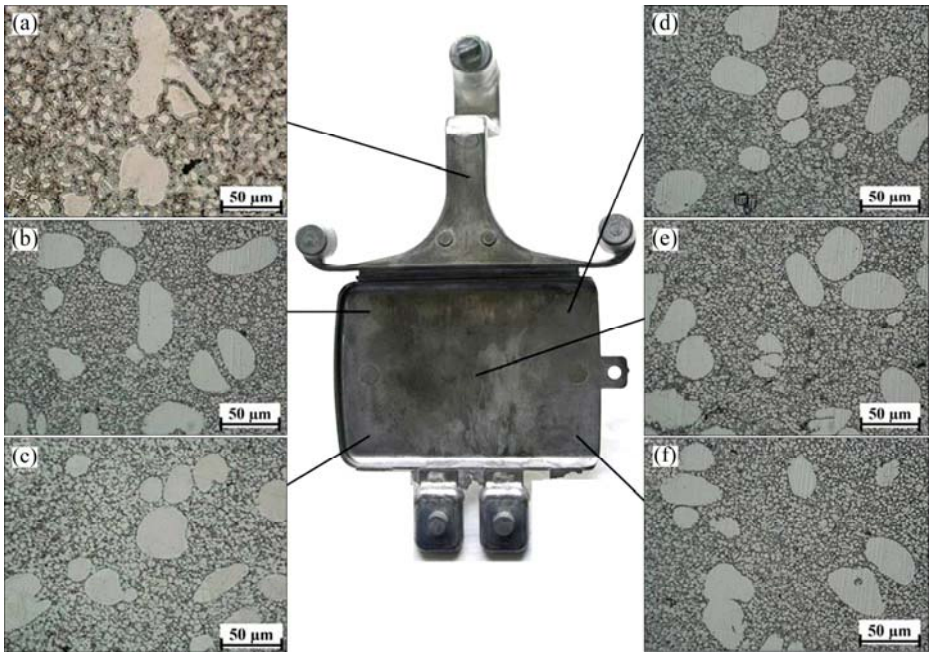

Fig. 5 Microstructures of phone cover fabricated by rheomoulding

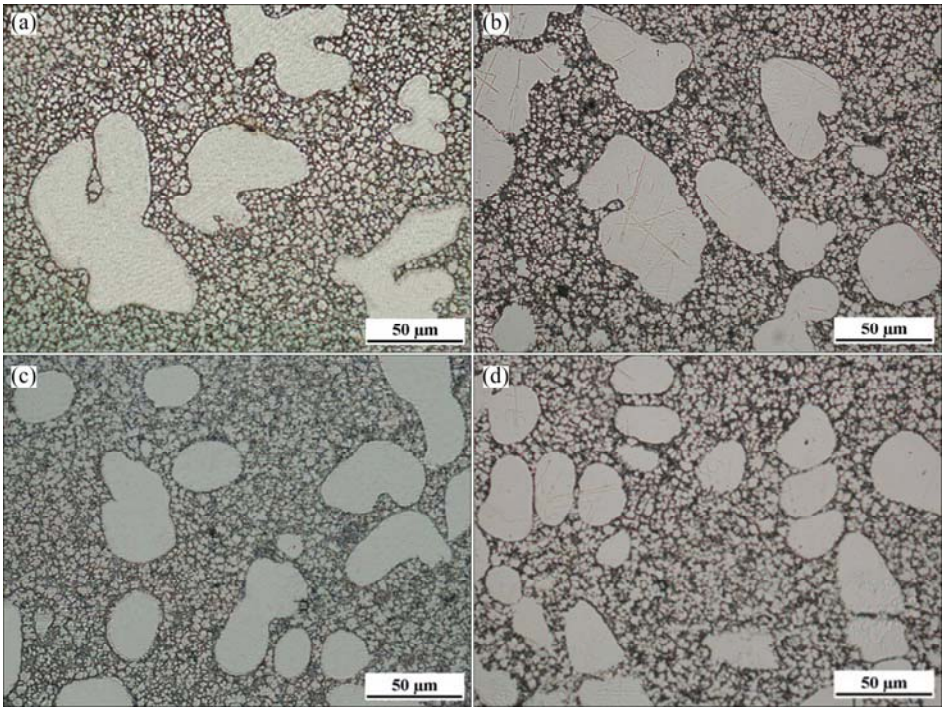

Fig. 6 Microstructures of rheomoulding phone covers at different pouring temperatures: (a) 635 °C; (b) 620 °C; (c) 610 °C; (d) 600 °C

Table 1 Quantitative analysis results of α-Mg and porosity fraction at different pouring temperatures

Pouring temperature/ °C	Average size/μm		Solid fraction/ %	Sphericity	Porosity fraction/ %
	α_1-Mg	α_2-Mg			
635	53.14	3.92	23.52	0.427	1.98
620	43.42	3.36	26.17	0.742	1.87
610	33.89	3.23	26.91	0.817	1.56
600	28.47	3.17	28.04	0.851	1.44

distributed in the matrix uniformly. The average size of α_1-Mg is 28.47 μm and the sphericity is 0.851. Furthermore, it is also found that α_2-Mg particles are slightly smaller with decreasing pouring temperature.

Figure 7 shows the mechanical properties of rheomoulding AZ91D under above conditions. Clearly, both the tensile strength and elongation increase dramatically with the decrease of pouring temperature. For HPDC, the tensile strength and elongation of AZ91D alloy are 212 MPa and 3.3%, respectively [21]. Compared with HPDC, both the strength and elongation of rheomoulding AZ91D reach or exceed them even if the pouring temperature is 635 °C.

It is well known that lowering the pouring temperature would promote the formation of equiaxed solidification [22−24]. Under the cooling effect of injection cylinder, the melt with low superheat maybe undercools quickly and abundant heterogeneous nucleation may occur throughout the slurry. This results

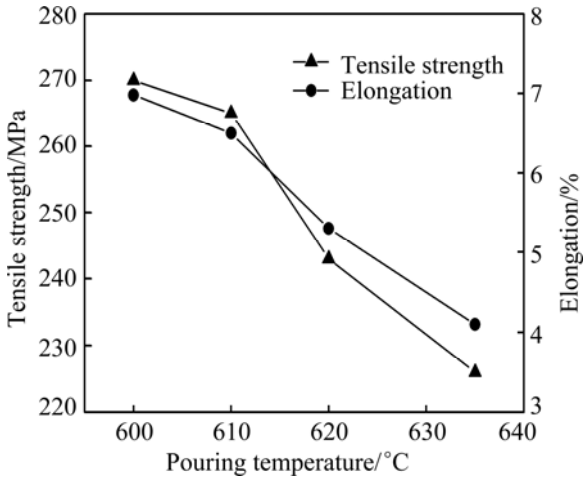

Fig. 7 Effects of pouring temperature on tensile strength and elongation

in the formation of numerous nuclei and the elimination of the columnar zone in the casting, and consequently, massive fine spherical α_1-Mg particles form (Fig. 6(d)). Meanwhile, a low pouring temperature would lead to the refinement of α_2-Mg due to the decrease of solidification time (Fig. 6(d)). It is believed that mechanical properties of rheoforming parts have a strong dependence on the microstructure morphology [5,25], and α_1-Mg with fine spherical features may be beneficial for parts to obtain good mechanical properties [5,10,25]. Also, the size of α_2-Mg, operating by means of the Hall−Petch equation, has already been recognized as an important factor determining the proof strength of casting Mg alloys [10],

and the smaller the α_2-Mg is, the better the strength is. Furthermore, decreasing pouring temperature would lead to a decrease in turbulence for high viscosity during the mold filling process and a reduction in casting defects for small solidification shrinkage, which have positive effects on mechanical properties [25,26]. Therefore, the best microstructure and mechanical property of rheomoulding AZ91D are obtained at a pouring temperature of 600 °C.

3.3 Effects of cylinder temperature on microstructure and mechanical property

Figure 8 shows microstructures of rheomoulding phone covers at cylinder temperatures of 595, 580, 565, 550, 535 and 520 °C, when the pouring temperature is 600 °C. The quantitative analysis results of α-Mg and the porosity fraction are listed in Table 2.

From Fig. 8 and Table 2, it is obvious that the cylinder temperature is essential for the solid fraction and the decrease of cylinder temperature is accompanied by the increase of solid fraction. It is also obvious that α_2-Mg particles are refined and the porosity fraction is evidently decreased with decreasing cylinder temperature. Furthermore, as the cylinder temperature decreases, the average size of α_1-Mg decreases firstly and then maintains relatively stable while the sphericity increases continuously. At 595 °C, α_1-Mg particles are not observed and there exist many porosities in rheomoulding AZ91D, as shown in Fig. 8(a). As the temperature decreases from 580 to 550 °C, α_1-Mg particles become fine and spherical gradually, as shown in Figs. 8(b−d). Finally, spherical and nearly spherical α_1-Mg particles are obtained at 535−520 °C though the size does not change too much, as shown in Figs. 8(e) and (f).

From the morphology evolution of α_1-Mg in Fig. 8, it can be concluded that a lower cylinder temperature is advantageous to obtain fine spherical α_1-Mg. Firstly, the

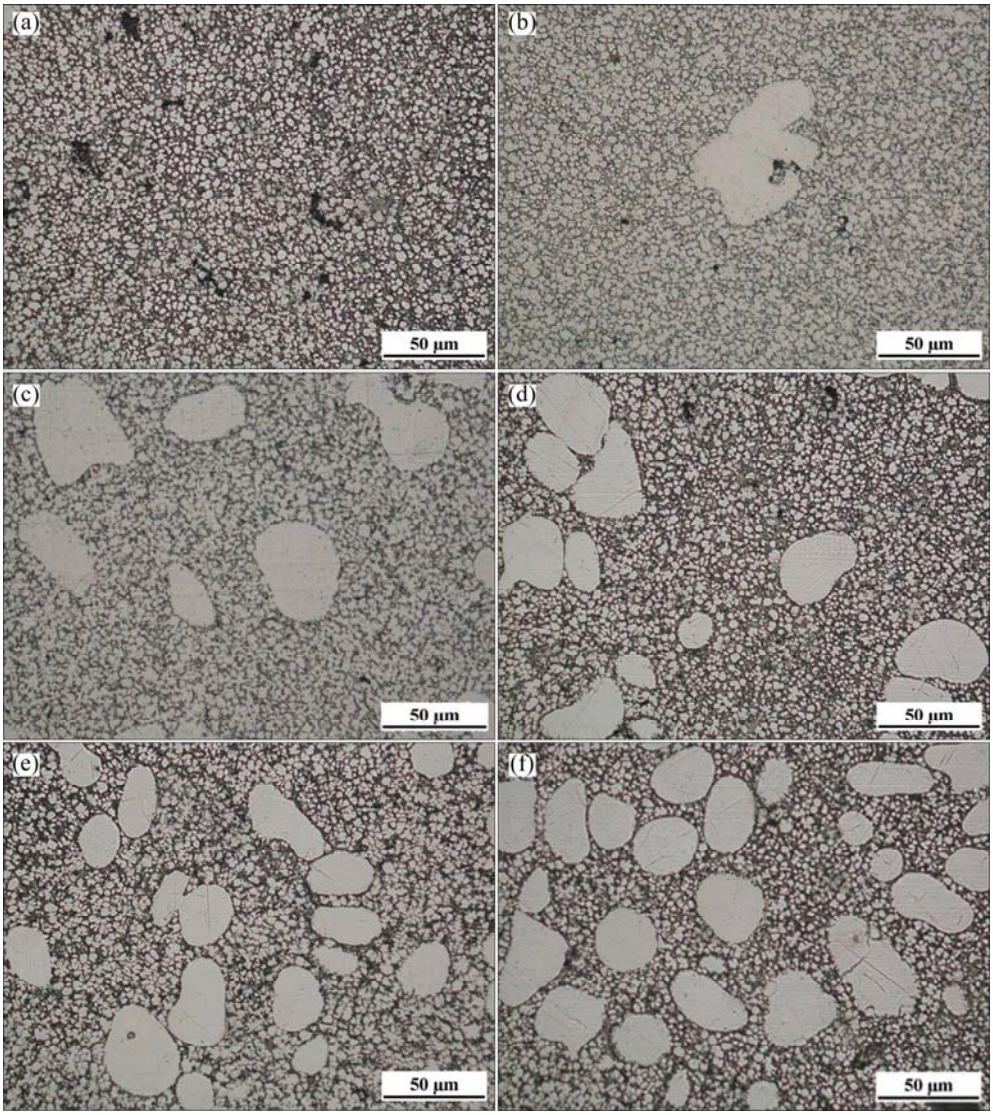

Fig. 8 Microstructures of rheomoulding phone covers at different cylinder temperatures: (a) 595 °C; (b) 580 °C; (c) 565 °C; (d) 550 °C; (e) 535 °C; (f) 520 °C

Table 2 Quantitative analysis of α-Mg and porosity fraction at different cylinder temperatures

Cylinder temperature/°C	Average size/μm		Solid fraction/%	Sphericity	Porosity fraction/%
	α_1-Mg	α_2-Mg			
595	−	3.89	0.00	−	2.11
580	58.22	3.83	5.01	0.542	1.73
565	40.39	3.72	10.92	0.768	1.58
550	32.51	3.31	19.78	0.821	1.55
535	27.67	3.23	24.56	0.853	1.61
520	29.11	3.15	34.27	0.876	1.65

critical nucleation radius and critical work decrease with lowering cylinder temperature for high cooling rate and large undercooling. Accordingly, the nucleation rate is increased and beneficial to obtaining fine α_1-Mg. Secondly, as the cylinder temperature decreases, the increase of solid fraction and the number of α_1-Mg decreases the distance among α_1-Mg particles, which could result in the increase of collision and friction frequency during injection, and as a further consequence finer and more spherical α_1-Mg particles are obtained. In addition, YANG et al [5,18] have shown that high α_1-Mg density is beneficial to the steadiness at solid−liquid interface and keeping α_1-Mg growing spherically. However, it should be noted that the cylinder temperature cannot be too low because excessively high cooling rate is adverse to α_1-Mg to keep the spherical morphology [8,22,27]. Furthermore, it should be pointed out that the mold cavity is not completely filled for low outlet temperature and poor liquidity when the cylinder temperature is below 490 °C in this study.

Figure 9 shows the effect of cylinder temperature on mechanical properties of rheomoulding AZ91D under above conditions. The results show that the cylinder

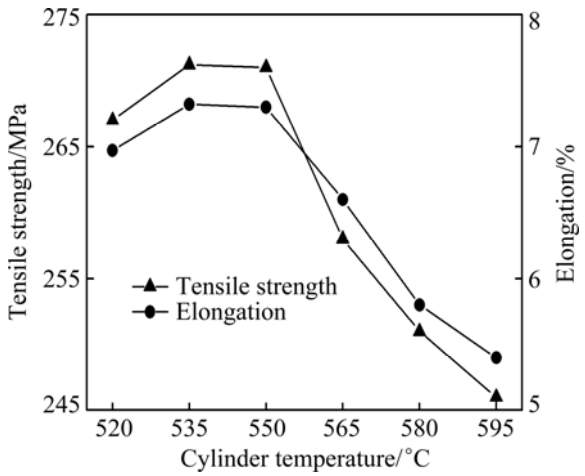

Fig. 9 Effects of cylinder temperature on tensile strength and elongation

temperature has a significant effect on mechanical properties of rheomoulding AZ91D. It is seen that the tensile strength and elongation increase as cylinder temperature decreases from 595 to 550 °C, but they only slightly change when the temperature is between 550 and 535 °C. While, as the temperature decreases further, both the tensile strength and elongation decrease suddenly.

To explain the mechanical property shown in Fig. 9, quantitative changes of porosity fraction and morphological changes of both phases during rheomoulding should be considered. It can be seen from Fig. 9 and Table 2 that, as the cylinder temperature decreases, the porosity fraction drastically decreases and α-Mg particles are obviously refined, which are especially beneficial to increasing mechanical properties of parts [21]. Mechanical properties of rheoforming AZ91D are mainly affected by two major phases: α-Mg and intermetallic β-$Mg_{17}Al_{12}$ [7,19,25]. A reduction in the cylinder temperature causes not only a refinement in size of α-Mg, but also a change in its internal microstructure [9−11]. Being a solid solution of Al and Zn in Mg, α-Mg particles are thought to be more susceptible to deformation than intermetallic β-$Mg_{17}Al_{12}$ which has higher strength and lower ductility [9,10,28]. Lowering forming temperature can increase the dislocation density in α_1-Mg and therefore strengthen their resistance to deformation, which would be conducive to enhance the strength of α_1-Mg by creating a drag force around the dislocations and then impeding their movement since the deformation of Mg−Al alloys at temperatures below 200 °C is interpreted by obstacle-controlled dislocation motion [9,28]. As the cylinder temperature decreases within the range of 595−550 °C, the strengthening of α_1-Mg, the refinement of α-Mg and the decrease of porosity fraction could compensate the reduction resulting from the increase of solid fraction, ensuring satisfying properties of rheomoulding AZ91D. However, a reduction in the strength and elongation, discovered below 535 °C of the cylinder temperature, indicates that the overall augments in strength are difficult to offset the reduction in strength resulting from the continuous increase of solid fraction.

Therefore, combining microstructures and mechanical properties, it can be concluded that the optimum cylinder temperature should be controlled between 550 and 535 °C. Under this condition, not only rheomoulding AZ91D alloy has desired microstructure and higher mechanical properties, but also energy is saved and the thermal shock to the mold is reduced.

3.4 Comparisons of mechanical properties under different processes

Table 3 lists mechanical properties of AZ91D alloy

parts under different processes as well as the average size of α-Mg. The ultimate tensile strength (UTS), yield strength (YS) and elongation of rheomoulding AZ91D fabricated at pouring temperature of 600 °C and cylinder temperature of 535 °C are 271 MPa, 169 MPa and 7.3%, respectively. Compared with thixomoulding and taper barrel rheo-diecasting, the UTS of rheomoulding is high, and both the YS and elongation rise. Compared with twin-screw rheo-diecasting, the UTS and YS of rheomoulding have a significant improvement though the elongation remains unchanged. Compared with HPDC, results indicate that the UTS, YS and elongation are increased by 27.8%, 15.7% and 121%, respectively.

Table 3 Mechanical properties and α-Mg size of AZ91D alloy parts under different processes

Process	Average size/μm		YS/ MPa	UTS/ MPa	Elongation/ %
	α_1-Mg	α_2-Mg			
Thixomoulding [28]	45.3	5.00	134	223	3.6
TBR rheo-diecasting [18]	46.0	12.57	128	225	4.5
Twin-screw rheo-diecasting [19]	40.9	6.00	145	246	7.4
HPDC [21]	51.3	−	146	212	3.3
Rheomoulding (this study)	27.7	3.23	169	271	7.3

Regardless of the influence of solid fraction on mechanical properties, such improvements of UTS, YS and elongation in rheomoulding AZ91D can be usually attributed to two main factors. One is the refinement of α-Mg. As shown in Table 3, the average size of α-Mg in rheomoulding AZ91D is far less than that under other processes. The other is less entrapped air and reduced shrinkage porosity. Porosity is an important structural factor of any casting and the porosity fraction of rheomoulding AZ91D fluctuates within the range of 1.44%−2.11% (Tables 1 and 2). While, for HPDC, the porosity fraction generally reaches 3.2% [16,29]. Factors that result in the decrease of mechanical properties in HPDC mainly involve gas porosities, microshrinkages, microstructural non-uniform and so on [3,5]. In HPDC process, coarse dendrites and microshrinkages would form at high pouring temperature during solidification, which results in microstructural coarseness and lower compactness of forming parts and worsens mechanical properties. While, in rheomoulding process, not only the pouring temperature is much lower than that of the HPDC and rheo-diecasting, but also the slurry is prepared by LSP instead of mechanical stirring. This contributes to greatly reducing the involvement of gas and the formation of defects. Based on above two factors, the refinement of α-Mg and the decrease of porosity ensure satisfactory mechanical properties of rheomoulding AZ91D.

4 Conclusions

1) The rheomoulding process can get rheomoulding AZ91D successfully in which α_1-Mg particles are fine, spherical and uniformly-distributed in the liquid matrix, and there are few porosities and no dendrites.

2) With the decrease of pouring temperature from 635 to 600 °C, the morphology of α_1-Mg changes from coarse rosette-like to fine spherical shape gradually, accompanied with the refinement of α_2-Mg and the decrease of the porosity fraction. This leads to an improvement in mechanical properties of rheomoulding AZ91D.

3) As the cylinder temperature decreases, the average size of α_1-Mg decreases firstly and then substantially maintains stable while the sphericity and solid fraction increase continuously. Also, the cylinder temperature has a significant effect on mechanical properties of rheomoulding AZ91D and the highest mechanical property is obtained at a cylinder temperature of 535 °C.

4) Rheomoulding AZ91D performs much better than thixomoulding, rheo-diecasting and HPDC in terms of mechanical properties. Compared with HPDC, the UTS, YS and elongation are increased by 27.8%, 15.7% and 121%.

References

[1] ZENG Y C, KE W, XU Y B. The latest development and application prospect of magnesium alloy [J]. Acta Metallurgica Sinica, 2001, 37: 673−685.

[2] WU Di, TANG Wei-neng, CHEN Rong-shi, HAN En-hou. Strength enhancement of Mg−3Gd−Zn alloy by cold rolling [J]. Transactions of Nonferrous Metals Society of China, 2013, 23(2): 301−306.

[3] JIANG J F, WANG Y, CHEN G, LIU J, LI Y F, LUO S J. Comparison of mechanical properties and microstructure of AZ91D alloy motorcycle wheels formed by die casting and double control forming [J]. Materials & Design, 2012, 40: 541−549.

[4] HEINE H J. Magnesium industry looks to the future [J]. Foundry Management & Technology, 1997, 4: 48−53.

[5] YANG Liu-qing, KANG Yong-lin, ZHANG Fan, XU Jun. Microstructure and mechanical properties of rheo-diecasting AZ91D Mg alloy [J]. Transactions of Nonferrous Metals Society of China, 2010, 20(S3): s862−s867.

[6] HOU W J, TAN J B, LIU J C. Research status and development trend of semisolid rheo-diecasting rheological [J]. Casting Technology, 2009, 30: 91−94. (in Chinese)

[7] GUAN Ren-guo, ZHAO Zhang-yong, CHAO Run-ze, ZHAO Hong-liang, LIU Chun-ming. Effects of technical parameters of continuous semisolid rolling on microstructure and mechanical properties of Mg−3Sn−1Mn alloy [J]. Transactions of Nonferrous Metals Society of China, 2013, 23(1): 73−79.

[8] FLEMINGS M C. Behavior of metals in the semi-solid state [J]. Metallurgical Transactions A, 1991, 22: 957−981.
[9] PATEL H A, CHEN D L, BHOLE S D, SADAYAPPAN K. Microstructure and tensile properties of thixomolded magnesium alloys [J]. Journal of Alloys and Compounds, 2010, 496: 140−148.
[10] ZHANG Y F, LIU Y B, CAO Z Y, ZHANG Q Q, ZHANG L. Mechanical properties of thixomolded AZ91D magnesium alloy [J]. Journal of Materials Processing Technology, 2009, 209: 1375−1384.
[11] GHOSH D, KANG K, ROEMER J G, VANSCHILT C, CARNAHAM R D. Properties and microstructure of thixomolded and heat treated AZ61A magnesium alloy [C]//Advances in Production and Fabrication of Light Metals and Metal Matrix Composites. Montreal, Canada: The Metallurgical Society of the CIM, 1992: 399−411.
[12] TSUKEDA T, TAKEYA K, SAITO K. Mechanical and metallurgical properties of shot molded AZ91D magnesium alloy [J]. Journal of Japan Institute of Light Metals, 1999, 47: 287−290.
[13] CZERWINSKI F. Near-liquidus molding of Mg−Al and Mg−Al−Zn alloys [J]. Acta Materialia, 2005, 53: 1973−1984.
[14] CZERWINSKI F. The processing phenomena of semisolid Mg−9%Al−l%Zn alloy at ultrahigh contents of the unmelted phase [J]. Materials Science and Engineering A, 2005, 392: 51−61.
[15] CZERWINSKI F. Magnesium alloy particulates for thixomolding applications manufactured by rapid solidification [J]. Materials Science and Engineering A, 2004, 367: 261−271.
[16] CUI Xiao-peng. The research on the microstructure and process of thixomolding AZ91D magnesium alloy [D]. Changchun: University of Jilin, 2006. (in Chinese)
[17] FAN Z T, HUANG N Y, LUO J R, WU S S. The new progress of semi-solid metal casting-injection molding [J]. Special Casting & Nonferrous Alloys, 2001, 2: 22−23. (in Chinese)
[18] YANG Liu-qing, KANG Yong-lin, ZHANG Fan, DING Rui-hua, LI Jiong. Rheo-diecasting of AZ91D magnesium alloy by taper barrel rheomoulding process [J]. Transactions of Nonferrous Metals Society of China, 2010, 20(6): 966−972.
[19] FAN Z. Development of the rheo-diecasting process for magnesium alloys [J]. Materials Science and Engineering A, 2005, 413−414: 72−78.
[20] WANG Y, XIA M, FAN Z, ZHOU X, THOMPSON G E. The effect of Al_8Mn_5 intermetallic particles on grain size of as-cast Mg−Al−Zn AZ91D alloy [J]. Intermetallics, 2010, 18: 1863−1869.
[21] PITSARIS C, ABBOTT T, DAVIES C H J, SAVAGE G. Influence of process parameters on the microstructure and mechanical properties of magnesium die castings [C]//Proceedings of the 6th International Conference on Magnesium Alloys and Their Applications. Weinheim: Wiley-VCH, 2003: 694.
[22] DONG J, CUI J Z, LE Q C, LU G M. Liquidus semi-continuous casting, reheating and thixoforming of a wrought aluminum alloy 7075 [J]. Materials Science and Engineering A, 2003, 345: 234−242.
[23] MI Guang-bao, LI Pei-jie, WANG Jing, HE Liang-ju. Formation and evolution of non-dendrite microstructure of Al−Si alloy slurry fabricated by near liquidus casting [J]. The Chinese Journal of Nonferrous Metals, 2011, 21(3): 560−69. (in Chinese)
[24] LE Q C, OU P, WU Y D, LU G M, CUI J Z, QIU Z X. Study on the near-liquidus casting of AZ91D magnesium alloy [J]. Acta Metallurgica Sinica, 2002, 38(2): 219−224.
[25] GUO Hong-min. Investigation on technique and theory of rheoforming for semi-solid aluminum alloys [D]. Nanchang: University of Nanchang, 2007. (in Chinese)
[26] TAO W L, ZHAO S D, LIN W J. Effects of processing parameters on thixo-diecasting box-type parts for automobile [J]. Special Casting & Nonferrous Alloys, 2011, 31(8): 687−690. (in Chinese)
[27] ZHANG Liang, WU Guo-hua, WANG Shao-hua, DING Wen-jiang. Effect of cooling condition on microstructure of semi-solid AZ91 slurry produced via ultrasonic vibration process [J]. Transactions of Nonferrous Metals Society of China, 2012, 22(10): 2357−2363.
[28] CZERWINSKI F, ZIELINSKA-LIPIEC A, PINET P J, OVERBEEKE J. Correlating the microstructure and tensile properties of a thixomolded AZ91D magnesium alloy [J]. Acta Materialia, 2001, 49: 1225−1235.
[29] LEE B D, BAEK U H, HAN J W. Optimization of gating system design for die casting of thin magnesium alloy-based multi-cavity LCD housings [J]. Journal of Materials Engineering and Performance, 2012, 21: 1893−1903.

浇注温度和缸体温度对 AZ91D 镁合金流变注射成形件组织及力学性能的影响

祁明凡[1]，康永林[1]，周 冰[1]，朱国明[1]，张欢欢[1]，李扬德[2]

1. 北京科技大学 材料科学与工程学院，北京 100083；2. 东莞宜安科技股份有限公司，东莞 523662

摘 要：介绍一种先进的集金属熔化、储存、浆料制备、浆料输送和注射成形于一体的流变注射成形机，并使用该设备生产一批 AZ91D 镁合金流变注射成形件。研究浇注温度和缸体温度对 AZ91D 镁合金流变注射成形件组织和力学性能的影响规律。结果表明，流变注射成形工艺可以成功获得初生 α-Mg 颗粒细小、圆整、均匀分布于基体组织中的 AZ91D 镁合金成形件。随着浇注温度的下降，初生 α-Mg 形貌由粗大的蔷薇状逐渐转变为细球状。随着缸体温度的降低，初生 α-Mg 颗粒的尺寸先下降，之后基本保持不变，其球形度和固相率不断提高。同时，适当地降低浇注温度或缸体温度可以细化 α-Mg 颗粒和降低孔隙率，这有助于流变注射成形件力学性能的提高。另外，AZ91D 镁合金流变注射成形件在力学性能上优于触变注射成形、流变压铸成形和高压铸造。与高压铸造相比，AZ91D 镁合金流变注射成形件的抗拉强度、屈服强度和伸长率分别提高了 27.8%、15.7%和 121%。

关键词：AZ91D 镁合金；流变注射成形；浇注温度；缸体温度；力学性能

(Edited by Xiang-qun LI)